

Analogues of Morphanthridine and the Tear Gas Dibenz[*b,f*][1,4]oxazepine (CR) as Extremely Potent Activators of the Human Transient Receptor Potential Ankyrin 1 (TRPA1) Channel

Harrie J. M. Gijzen,^{*,†} Didier Berthelot,[†] Mirko Zaja,^{†,§} Bert Brône,^{‡,||} Ivo Geuens,[‡] and Marc Mercken[‡]

[†]*Medicinal Chemistry Department and* [‡]*Neuroscience, Johnson & Johnson Pharmaceutical Research & Development, Turnhoutseweg 30, 2340 Beerse, Belgium.* [§]*Current affiliation: 4SC AG, Am Klopferspitz 19a, 82152 Planegg, Martinsried, Germany.* ^{||}*Current affiliation: BIOMED Research Institute, Hasselt University, Agoralaan, Bld C, B-3590 Diepenbeek, Belgium.*

Received April 19, 2010

The TRPA1 channel can be considered as a key biological sensor to irritant chemicals. In this paper, the discovery of 11*H*-dibenz[*b,e*]azepines (morphanthridines) and dibenz[*b,f*][1,4]oxazepines is described as extremely potent agonists of the TRPA1 receptor. This has led to the discovery that most of the known tear gases are potent TRPA1 activators. The synthesis and biological activity of a number of substituted morphanthridines and dibenz[*b,f*][1,4]oxazepines have given insight into the SAR around this class of TRPA1 agonists, with EC₅₀ values ranging from 1 μM to 0.1 nM. Compounds **6** and **32** can be considered as the most potent TRPA1 agonists known to date, with **6** now being used successfully as a screening tool in the discovery of TRPA1 antagonists. The use of ligands such as **6** and **32** as pharmacological tools may contribute to the basic knowledge of the TRPA1 channel and advance the development of TRPA1 antagonists as potential treatment for conditions involving TRPA1 activation, including asthma and pain.

Introduction

The transient receptor potential ankyrin 1 (TRPA1,^a formerly named ANKTM1) receptor belongs to the transient receptor potential (TRP) family of cation-selective channels which have been shown to transduce mechanical, thermal, and pain-related inflammatory signals.¹ Within this family, the TRPA1 receptor appears to play a key role as a biological sensor and has been implicated in a growing number of pathophysiological conditions,² such as neuropathic or inflammatory pain,³ airway diseases,⁴ and bladder disorders.⁵ The TRPA1 channel is activated by a number of pungent chemicals, such as allyl isothiocyanate (**1**, AITC) present in mustard oil, diallyl thiosulfinate (**2**, allicin) present in garlic, and cinnamaldehyde (**3**) present in cinnamon (Chart 1).⁶ A comprehensive overview of reported TRPA1 agonists can be found in a recent article^{1b} and includes phytochemicals, environmental derived irritants, a variety of medicines, and endogenously produced reactive reagents. Although several nonelectrophilic agents, such as thymol and menthol, have been reported as TRPA1 agonists, most of the known activators are electrophilic chemicals which have been shown to activate the TRPA1 receptor via the formation of a reversible

covalent bond with cysteine residues present in the ion channel.⁷ The reported potencies of the various agonists range from 1 to 100 μM, with the most potent members of a particular class displaying activities in the low to submicromolar range.^{1b} For example, **3** has a reported EC₅₀ of 19 μM while an analogous isatin derived cinnamide, dubbed “supercinnamaldehyde” in the same assay, had an EC₅₀ of 0.8 μM.^{7b}

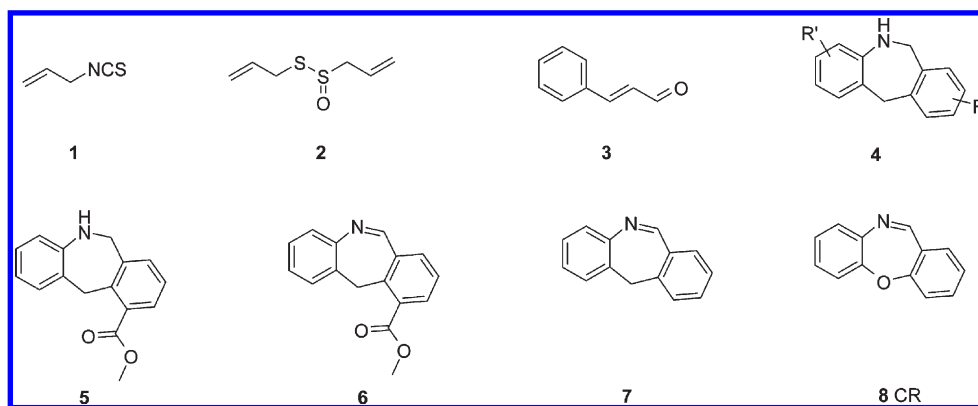
In a high throughput screen aimed at the identification of TRPA1 ligands, a family of hits was discovered to behave as moderate to potent agonists of the TRPA1 receptor. They all belonged to a class of tricyclic 6,11-dihydro-5*H*-dibenz[*b,e*]azepines or 5,6-dihydromorphanthridines of general structure **4** and exemplified by compound **5** (Chart 1). During resynthesis of compound **5** for hit confirmation, the compound was found to be rather unstable and to be partly oxidized to the corresponding morphanthridine **6** on prolonged standing in solution and exposure to air. In addition, upon handling of the oxidized compound, laboratory personnel noticed a pungent, irritating effect on eyes and nose. Isolation of pure **6** and subsequent in vitro testing showed the compound to be an extremely potent agonist of the human TRPA1 receptor with an EC₅₀ of 0.1 nM, a 1000-fold increase in potency over the previously known agonists such as **1**.^{1,2} A careful reanalysis of the original DMSO solutions used in the HTS campaign revealed that 1–5% of compound **5** had indeed been converted into **6**. Also, in all of the analogous 5,6-dihydromorphanthridine hits **4**, varying amounts of oxidized product could be detected. Obviously, with a subnanomolar potency, trace amounts of morphanthridine present would already result in a considerable measured activity. The parent, unsubstituted morphanthridine **7** was also shown to be a potent agonist of the TRPA1 receptor with an EC₅₀ of 3 nM.

The structural resemblance of the morphanthridine tricyclic moiety with dibenz[*b,f*][1,4]oxazepine (**8**, CR), which is one of

^{*}To whom correspondence should be addressed. Phone: +32-14-606830. Fax: +32-14-5344. E-mail: hgijzen@its.jnj.com.

^aAbbreviations: A/F, ampere/farad; AITC, allyl isothiocyanate; BITC, benzyl isothiocyanate; CA (BBC), bromobenzyl cyanide; CN, 1-chloroacetophenone; CR, dibenz[*b,f*][1,4]oxazepine; CS, 2-chlorobenzylidene malononitrile; FDSS, functional drug screening system; HEK293, human embryonic kidney 293; I/Cslow, current/slow component of membrane capacitance; IC₅₀, concentration that will incapacitate 50% of the population exposed to the tear gas for a specific period; TC₅₀, threshold concentration with effect on 50% of population after 1 min of exposure; TRP, transient receptor potential; TRPA1, transient receptor potential ankyrin 1; cTRPM8, canine transient receptor potential melastatin 8; hTRPV1, human transient receptor potential vanilloid 1.

Chart 1

**Table 1.** Tear Gases as TRPA1 Agonists: Potencies as a Result of Fluorometric (FDSS) Studies Compared with the Human in Vivo Efficiency of the Tear Gases^{9,a}

Nr.	Name/Code	Structure	hTRPA1 EC ₅₀ FDSS (nM)	TC ₅₀ (mg/m ³)	IC ₁₅₀ (mg.min/m ³)
1	AITC		398		
7	Morphanthridine		3		
8	CR		0.3	0.004	0.7
9	CN		30	0.3	20-50
10	CS		0.9	0.004	3.6
11	CA (BBC)		10	0.3	30

^aTC₅₀: threshold concentration with an effect on 50% of population after 1 min of exposure. IC₁₅₀: concentration that will incapacitate 50% of the population exposed to the tear gas for a specific period.

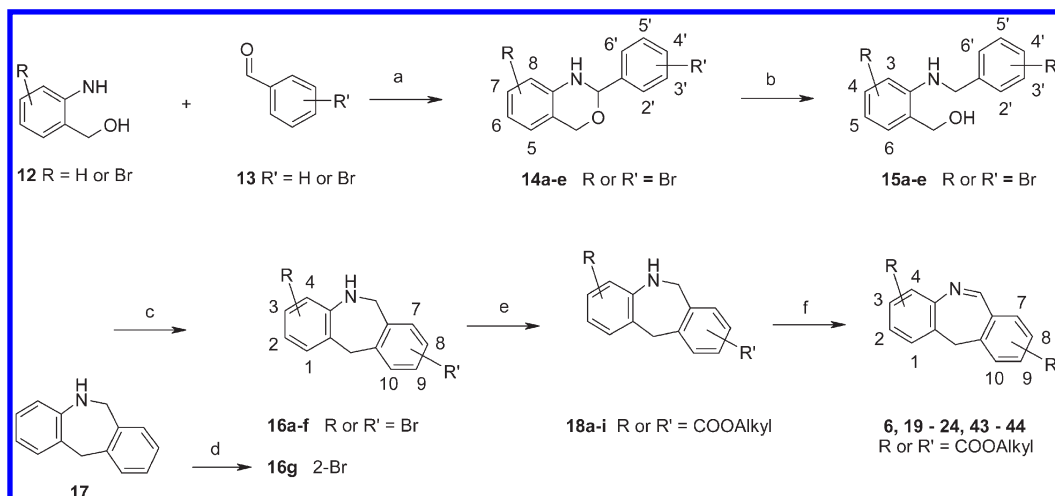
the ingredients found in currently used tear gases, also known as riot control or incapacitating agents, has led to the discovery of the mechanism of action for most of the tear gases used today and in the past.⁸ For the tear gases **8** (CR), 1-chloroacetophenone (**9**, CN), 2-chlorobenzylidene malononitrile (**10**, CS), and bromobenzyl cyanide (**11**, CA or BBC), a good correlation has been observed between the relative in vitro TRPA1 potencies with their reported human in vivo efficiencies as tear gases⁹ as shown in Table 1. Recently, behavioral tests in mice, either using TRPA1 deficient mice or treating normal mice with TRPA1 antagonists, have confirmed the central role of TRPA1 in the involuntary nocifensive reflex responses to tear gas agents.¹⁰

Most of the TRPA1 agonists known today, including the tear gases such as **8**, **9**, and **10**, have in common an electrophilic carbon or sulfur that can be subject to nucleophilic attack by thiol (cysteine) or amine (lysine) groups, present in the TRPA1 receptor, and can form a covalent interaction with the receptor.⁷ The variety of structures in this group of electrophilic agents illustrates that chemical reactivity in combination with a lipophilicity enabling membrane permea-

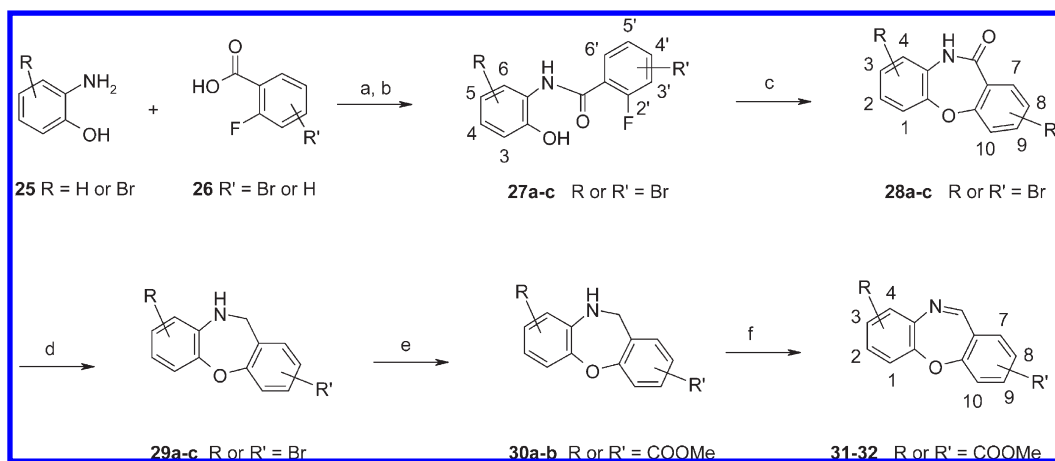
tion is crucial to their TRPA1 receptor agonistic effect.⁶ In this paper we describe the SAR around this dibenz(ox)azepine tricyclic class of TRPA1 agonists and demonstrate that, in addition to the requirement of an electrophilic functionality, noncovalent interactions with the receptor also play a role in the potency of these compounds.

Chemistry

All the final dibenz(ox)azepine compounds were prepared via oxidation of the corresponding dihydro derivatives. The synthesis of **6** and the carboxylic ester substituted 11*H*-dibenz[*b,e*]azepines (morphanthridines) analogues is depicted in Scheme 1.¹¹ Condensation of *o*-aminobenzyl alcohol **12** with benzaldehyde **13** gave the bromo-substituted 2-phenyl-1,4-dihydro-2*H*-benz[*d*][1,3]oxazines **14a–e** in quantitative yield. Reductive cleavage with NaBH₄ in ethanol afforded [2-benzylaminophenyl]methanol intermediates **15a–e**. The 3-bromo derivative **15b** was prepared via a slightly modified procedure by performing a reductive amination between benzaldehyde and *O*-acetyl-3-bromo-2-aminobenzyl alcohol, followed by

Scheme 1^a

^a Reagents and conditions: (a) ^tPrOH; (b) NaBH₄, EtOH; (c) CH₂Cl₂, H₂SO₄; (d) Br₂, HOAc; (e) Pd(OAc)₂, dppp, K₂CO₃, MeOH, THF, 50 atm of CO, 125 °C; (f) MnO₂, toluene or air oxidation.

Scheme 2^a

^a Reagents and conditions: (a) SOCl₂; (b) Et₃N, THF; (c) NaOH, DMF; (d) LiAlH₄, or BH₃, THF; (e) Pd(OAc)₂, dppp, K₂CO₃, MeOH, THF, 50 atm of CO, 125 °C; (f) MnO₂, toluene.

hydrolysis of the acetyl protecting group (not shown). Intermediates **15a–e** were cyclized to the desired 6,11-dihydro-5H-dibenz[*b,e*]azepines **16a–f** with sulfuric acid using dichloromethane as cosolvent. For the 3'-bromo derivative **15a**, this resulted in a mixture of 10- and 8-bromo derivatives **16a** and **16b**, respectively. For all other intermediates **15b–e**, the corresponding brominated 6,11-dihydro-5H-dibenz[*b,e*]azepines **16c–f** were obtained as single regioisomers. The 2-bromo derivative **16g** was prepared more easily via regioselective bromination of the readily available 6,11-dihydro-5H-dibenz[*b,e*]azepine **17**. Subsequently, the bromo derivatives **16a–g** were converted into carboxylic esters **18a–i** followed by oxidation to the desired dibenz[*b,e*]azepines. This final oxidation was routinely carried out using an excess of MnO₂ in toluene. Upon prolonged standing in aqueous solution, ranging from hours to days, oxidation of the 6,11-dihydro-5H-dibenz[*b,e*]azepines to the corresponding dibenz[*b,e*]azepines was observed. This became apparent especially during lengthy preparative reversed phase HPLC purifications and was used to our advantage in the isolation of a number of final compounds, such as 8-bromo derivative **24**.

The general synthesis of the dibenz[*b,f*][1,4]oxazepine carboxylic esters is depicted in Scheme 2. Benzamide formation

between anilines **25** and benzoic acids **26** followed by intramolecular S_NAr reaction installed the required tricyclic ring system. Reduction of the dibenzo[*b,f*][1,4]dioxepanones **28a–c** gave the brominated 10,11-dihydrodibenz[*b,f*][1,4]oxazepines **29a–c**, which were converted to the required target compounds **31–32** in analogy to the synthesis of the dibenz[*b,e*]azepines.

Several of the brominated dihydro intermediates **16** and **29** were also used to synthesize derivatives bearing a variety of substituents. Direct oxidation of intermediates 8- and 10-bromo derivatives **16b** and **16a** gave bromo analogues **34** and **35**, respectively (Scheme 3). Cyano- and carboxamide-substituted dibenz(ox)azepine derivatives **36–39** and **40–42**, respectively, were prepared starting from the corresponding bromo derivatives as exemplified in Scheme 3.

Carboxylic acid derivative **46** was prepared via basic hydrolysis of **18a** (Scheme 4). The intermediate acid **45** was directly oxidized to **46** during the extended hydrolysis reaction time (3 days). Carboxylic acid **45** was also formed via a CO insertion reaction of **16a** in the presence of water. Again, intermediate **45** was not isolated but immediately reacted to form methoxypropylamide **47**, which was subsequently oxidized to give compound **49**. The diethylamide analogue **50** was obtained

directly in low yield via a CO insertion reaction of **16a** in the presence of diethylamine. Oxidation of intermediate **48** took place during the reversed phase HPLC purification leading to **50**.

Biology

Primary in Vitro Functional Assay. All compounds were tested using Ca^{2+} fluorometry. Binding of an agonist to the TRPA1 ion channel opens the ion channel which causes a robust increase in intracellular Ca^{2+} concentration. For detecting and measuring intracellular Ca^{2+} concentration, hTRPA1 transfected HEK293 cells were loaded with a Ca^{2+} -sensitive dye (Fluo4-AM, Molecular Probes, Invitrogen, Belgium). Changes in fluorescence in the cell that

correspond to changes in Ca^{2+} concentration in the cell can kinetically be monitored with the FDSS instrument (Hamamatsu) and are indicative for agonism toward the TRPA1 ion channel. The results are expressed as EC_{50} representing the molar concentration of the compound, which resulted in 50% of the maximal increase in Ca^{2+} concentration. Each quoted value is the mean of at least four experiments. Further biological experiments are explained in the next section.

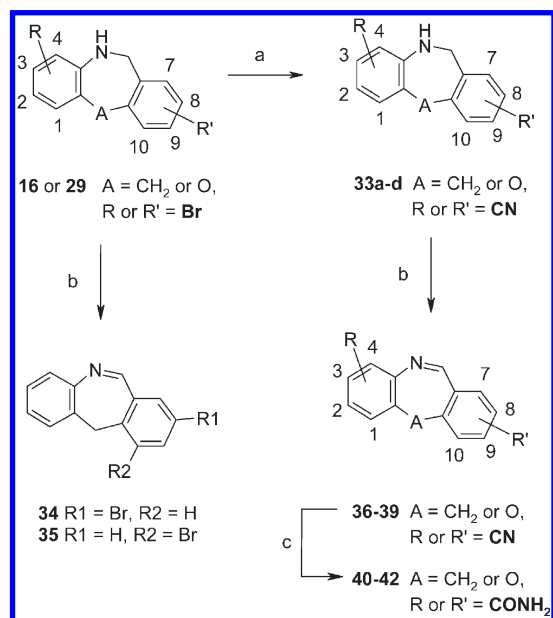
Results and Discussion

Commercially available and structurally related but nonelectrophilic, tricyclic analogues of morphanthridine (**7**) or **8**, such as **51**, **52**, and fluperlapine (**53**) were tested and found to be inactive ($\text{EC}_{50} > 5 \mu\text{M}$) (Chart 2). Substitution of the electrophilic carbon in **8** with a methyl group, giving compound **54**, also sufficed to suppress the agonistic activity completely. Incubation of **54** with benzylmercaptane as a thiol nucleophile, mimicking the cysteine residues in the TRPA1 receptor, did not show any formation of adduct, in contrast to similar experiments with **8**.⁸ The inactivity of phenanthridine (**55**) illustrates further the need for an electrophilic carbon.

The presence of an unsubstituted, electrophilic, disubstituted imine is no guarantee for activity. Benzalaniline (**56**) was shown to react rapidly with thiols such as benzylmercaptan but was totally devoid of activation of the hTRPA1 receptor. For **56**, the orientation of the two phenyl groups may prohibit the positioning of the imine functionality in the proximity of the cysteine thiols of the ion channel, hence preventing covalent binding and activation of the receptor. The sulfur analogue dibenzo[*b,f*][1,4]thiazepine (**57**) did activate the TRPA1 receptor with an EC_{50} of 9 nM. Again, this compound has been described as being extremely irritating to the skin, mucous membranes, and eyes.¹² None of the inactive compounds **51**–**56** were able to block the action of **6** or other TRPA1 agonists, and they can therefore be considered also to be devoid of hTRPA1 antagonistic activity.

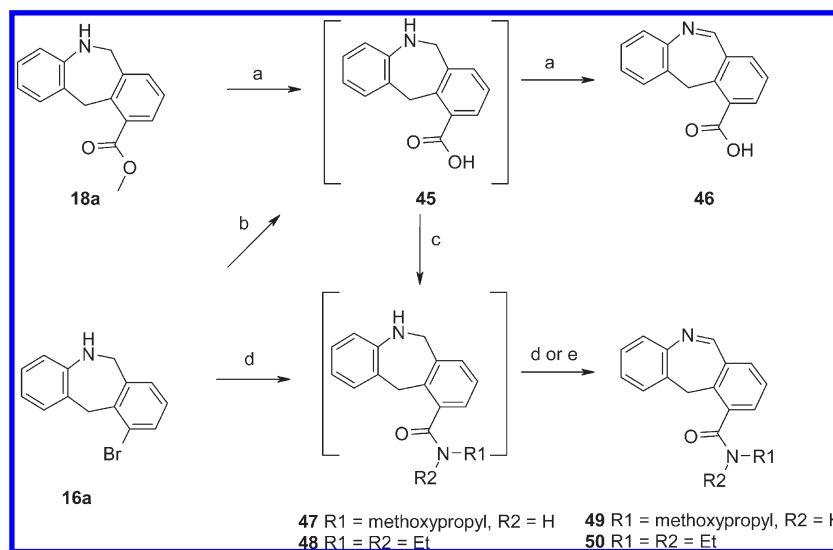
The data for the compounds in Charts 1 and 2 confirm the requirement of a thiol-reactive electrophilic component,

Scheme 3^a



^a Reagents and conditions: (a) CuCN, DMF, 140 °C; (b) MnO₂, toluene; (c) H₂SO₄.

Scheme 4^a



^a Reagents and conditions: (a) LiOH, THF/H₂O; (b) Pd(OAc)₂, dppp, THF, Et₃N, H₂O, 50 atm of CO, 150 °C; (c) methoxypropylamine, HBTU; (d) Pd(OAc)₂, dppp, THF, Et₃NH, 50 atm of CO, 150 °C; (e) MnO₂, toluene.

Chart 2

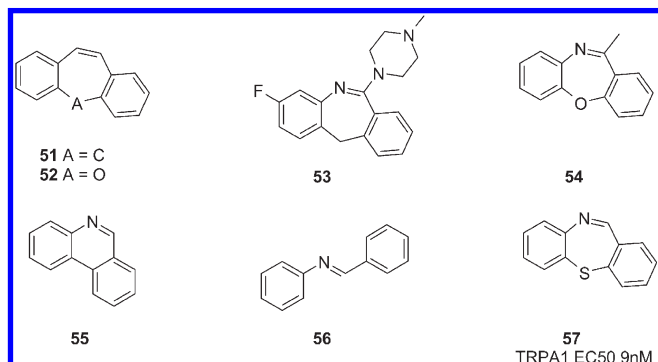
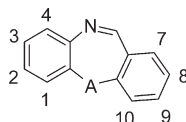


Table 2. Activity of Carboxylic Ester Substituted Dibenz(ox)azepine Analogues



compd	substituent	A	TRPA1 EC ₅₀ (nM)
7	H	CH ₂	3
19	1-COOMe	CH ₂	0.6
20	2-COOMe	CH ₂	0.4
21	3-COOMe	CH ₂	19
22	4-COOMe	CH ₂	31
23	7-COOMe	CH ₂	31
24	8-COOMe	CH ₂	100
31	9-COOMe	O	6
32	10-COOMe	O	0.05
6	10-COOMe	CH ₂	0.1

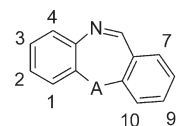
as observed in most exogenous and endogenous TRPA1 activators.^{1b} In addition, it illustrates that this electrophilic moiety needs to be accessible to the cysteine thiol groups in the TRPA1 receptor. This creates the possibility to further optimize the interaction of the benzo(ox)azepines class of TRPA1 agonists via structural modification.

The influence of substitution of the dibenz(ox)azepine tricyclic core was investigated via a series of morphanthridine and CR analogues containing various substituents on all of the eight possible aryl carbon positions.

The potencies of a set of carboxylic methyl ester substituted derivatives are given in Table 2. Although all of the synthesized analogues were shown to activate the TRPA1 receptor, the large differences in potencies point toward additional interactions with the receptor. This is best illustrated by the 1000-fold potency difference between compounds **6** and **24**. In both compounds, the carboxylic methyl ester substituents are oriented in a meta fashion to the electrophilic imine carbon atom, thus resulting in a comparable influence on the electrophilic nature of this carbon. The influence on the potency of the carboxylic ester substituents on the 8- and 10-position can therefore only be explained via additional, noncovalent interactions with the TRPA1 receptor.

In general, 1-, 2-, and 10-substituted compounds showed the highest potencies (Table 2, compounds **19**, **20**, **32**, and **6**), with CR analogue **32** being the most potent compound discovered so far, having an EC₅₀ of 50 pM. Overall, substitution in proximity to the electrophilic imine moiety (compounds **21–24**) resulted in a lower activity than substitution away

Table 3. Activity of Substituted Dibenz(ox)azepine Analogues



compd	substituent	AAA	hTRPA1 EC ₅₀ (nM)
34	8-Br	CH ₂	33
35	10-Br	CH ₂	3.5
36	8-CN	CH ₂	158
37	10-CN	CH ₂	1.6
38	10-CN	O	0.15
39	1-CN	O	0.10
40	10-CONH ₂	CH ₂	2.5
41	10-CONH ₂	O	0.08
42	1-CONH ₂	O	0.11
43	8-COO'Pr	CH ₂	933
44	10-COOnBu	CH ₂	6.2
46	10-COOH	CH ₂	245
49	10-CONH(CH ₂) ₃ OMe	CH ₂	7.7
50	10-CONEt ₂	CH ₂	40
58	9-OMe	O	14
59	9-OH	O	2.1

from the reactive center, indicating that steric interactions close to the reactive cysteine thiol groups of the ion channel are the determining factor for the potency in this class of TRPA1 activators.

Further variation on substituents was investigated as shown in Table 3. To confirm the difference in activity of 8- vs 10-substituted analogues, the 8-bromo and 8-cyano derivatives were also prepared and tested. The 8-bromo derivative **34** showed a 10-fold decrease in activity compared to the 10-bromo analogue **35**. For the 8- and 10-cyano derivatives **36** and **37**, a 100-fold difference in activity was observed. Cyano substituted dibenz[*b,f*][1,4]oxazepines **38** and **39** were among the most potent analogues synthesized and confirm the data from Table 2, indicating that the 1- and 10-positions are the optimal places for substitution, as well as the increased potency for dibenzoxazepines compared to dibenzazepines. An increase in size of the 8-substituent, such as in isopropyl carboxylic ester substituted **43**, resulted in a further decrease in activity compared to methyl ester **24**. This is in line with the hypothesis that (lack of) steric hindrance is the main driver for potency. Larger substituents on the 10-position such as in compounds **44**, **49**, and **50** also resulted in reduced potency but still retained significant activity. This may provide a handle to work on druglike properties such as aqueous solubility.

As mentioned above, most of the known TRPA1 agonists are lipophilic compounds, which is in agreement with the low activity for carboxylic acid **46**. On the other hand, carboxamides **40–42** displayed a similarly high potency as their cyano analogues **37–39**. The hydroxy- and methoxy-substituted morphanthridines **58** and **59** were prepared and tested, since their irritant properties have been described before.¹³ The methoxy derivative **58** has been described as highly irritant, whereas in the same study the hydroxyl analogue **59** did not show any irritant properties. Surprisingly, in our hands, the hydroxy-substituted **59** showed a more potent in vitro activation of the TRPA1 receptor than **58**. A possible explanation for this in vitro/in vivo discrepancy could be the lower membrane permeability of the more polar **59** compared to **58**. Patch-clamp electrophysiology experiments have shown that chemical activators of TRPA1 need to traverse

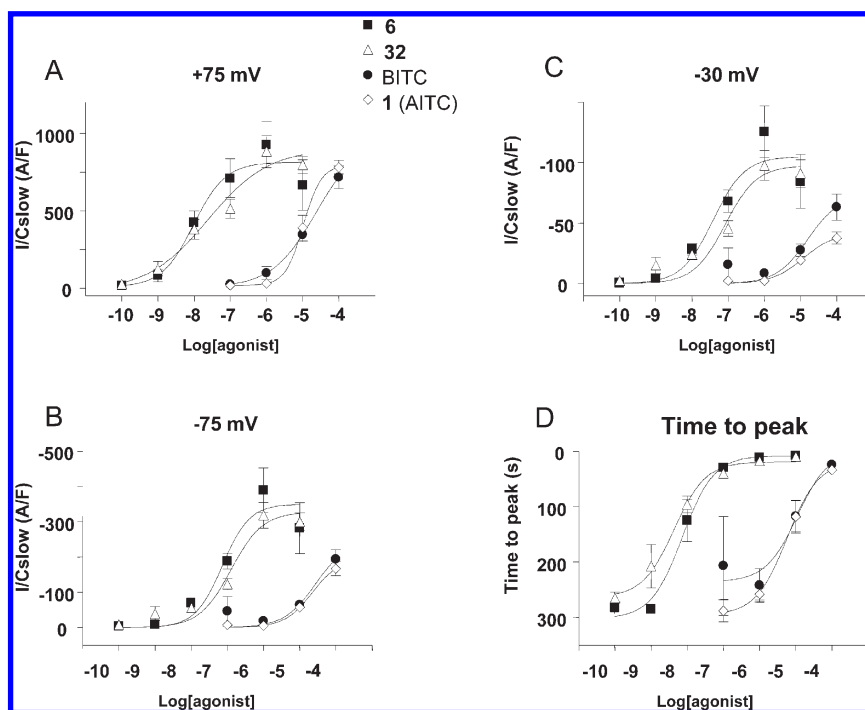


Figure 1. Concentration response graphs of TRPA1 agonists in electrophysiological measurements. In panels A and B the hTRPA1 current density, measured at 75 and -75 mV, respectively, was plotted as a function of the concentration of the different agonists. Panel C shows the current density measured at a holding potential of -30 mV. The current density was calculated by normalizing the currents to the slow component of membrane capacitance (I/C_{slow}), measured (ampere/farad: A/F) during the experiment. Note that the I/C_{slow} has negative values when measured at -30 and -75 mV because these are inward currents. In panel D the time to peak is shown as a function of concentration. The time to peak is the time between the application of the agonist and time point of the maximal current amplitude, with a maximum of 300 s. Every data point represents the mean and SEM of five to nine replicates for **6** and **32** and three to six replicates for AITC (**1**) and BITC.

the plasma membrane to activate the ion channel.¹⁰ In the same study, the requirement of cysteine residues present in the cytosolic, N-terminal domain of the TRPA1 receptor was demonstrated by the lack of activation by **8** and other tear gases of mutant TRPA1 channels.

In order to confirm the effect of the compounds on TRPA1, whole cell voltage clamp experiments were performed for compounds **6** and **32** in comparison to the known agonists AITC (**1**) and benzylisothiocyanate (BITC), using the methodology as described previously⁸ (Figure 1).

The concentration response curves at the three membrane potentials are plotted in Figure 1A–C. In addition, the time to peak of the same current maxima was plotted as concentration response curves in Figure 1D. The pEC_{50} values obtained from the fitting procedure are shown in Table 4. A membrane potential of -30 mV is probably the most relevant membrane potential because activated (i.e., open) TRPA1 channels will force the resting membrane potential of a cell toward the equilibrium potential of the TRPA1 channel (i.e., -10 to 0 mV in a physiological environment).

These results confirm that **6** and **32** are potent TRPA1 agonists. The potencies of AITC and BITC are hard to determine because of solubility problems at higher concentrations. The plateau phase of the concentration response relationships has not been reached, but we can at least conclude that their EC_{50} values will be above the micromolar range.

To check the selectivity of this class of TRPA1 agonists, we investigated the cross-selectivity on hTRPV1 (which is the target for the capsaicin-containing pepper sprays) and cTRPM8¹⁴ on compounds **6**, **7**, and **8**.¹⁵ No agonism was found on either hTRPV1 or cTRPM8, confirming their TRPA1 selectivity (data not shown).

Table 4. Effect of the TRPA1 Agonists on Currents Measured at Different Membrane Potentials and on the Time to Peak^a

	AITC (1)	BITC	6	32
-75 mV	4.65 ± 0.75	4.56 ± 0.24	7.14 ± 0.20	6.90 ± 0.16
-30 mV	4.92 ± 0.17	4.81 ± 0.25	7.42 ± 0.22	7.08 ± 0.17
75 mV	4.98 ± 0.12	4.62 ± 0.97	8.01 ± 0.37	7.62 ± 0.38
time to peak	5.24 ± 0.19	4.96 ± 0.40	8.36 ± 0.14	8.13 ± 0.11

^a The pEC_{50} values from the concentration response curves in Figure 1 are compared ($-\log[\text{agonist}]$, mean \pm SEM). The pEC_{50} values of the different agonists at -30 mV were significantly different ($p \leq 0.05$; F -test).

Upon incubation of the ester derivatives **6** and **32** with human liver microsomes at a $5 \mu\text{M}$, complete conversion was observed to the corresponding acids within 15 min of treatment. After prolonged (7 h) incubation under similar conditions but in the absence of liver microsomes, no degradation was observed, demonstrating the chemical stability of compounds **6** and **32**. The chemical stability also became apparent upon accidental, minimal contamination of the hands with these compounds, which 24 h later was still capable of inducing strong lachrimation upon hand–eye contact.

Incubation with liver microsomes in the presence of glutathione and subsequent analysis of the mixture for the presence of glutathione adducts are a commonly used technique in drug discovery to detect the formation of reactive intermediates.¹⁶ When compounds **6**, **8**, and **32** were added to a solution containing liver microsomes and glutathione, no parent or metabolite–glutathione adducts were observed after 1 h of incubation for **6** or **32** while at least five different adducts could be detected for **8**.¹⁷ No glutathione adduct formation was observed in the absence of human liver microsomes under the same incubation conditions, indicating the

need for metabolic activation before covalent binding of **8** to glutathione. The lack of formation of reactive intermediates or observation of parent–glutathione adducts for **6** and **32** could result in a reduced toxicity profile of these compounds compared to **8**. The use of ester-substituted analogues of **8** as incapacitating (tear gas) agents may therefore lead to an improved safety profile. The currently used tear gases CR and CS have been described as environmentally persistent chemicals, which can also be countered via the introduction of carboxylic acid ester substituents by increasing aqueous solubility and hydrolytic degradation. Further research into the structure–activity relationship of these TRPA1 agonists may lead to more safe and environmentally friendly alternatives for the currently used tear gases.

The work described in this paper has led to the identification of the most potent class of TRPA1 agonists known today. The results confirm the observation of thiol-reactive electrophiles being able to activate the TRPA1 receptor. In addition, the inactivity of benzalaniline (**56**) and the SAR around the benzo(ox)azepines demonstrate the importance of an optimal fit of the electrophiles within the TRPA1 receptor in order to achieve maximal potency.

Compound **6** has now been used successfully as a screening tool in the discovery of TRPA1 antagonists.¹⁸ Data obtained using **6** were comparable to the use of the more commonly used but less potent isothiocyanate TRPA1 agonists such as benzyl isothiocyanate, with the advantage of giving a more robust signal. The SAR results and the use of ligands such as **6** and **32** as pharmacological tools may contribute to the basic knowledge of the TRPA1 channel and facilitate the discovery of new treatments for diseases such as asthma and pain.

Experimental Section

Chemistry. Melting points were determined with a DSC823e (Mettler-Toledo) and were measured with a temperature gradient of 30 °C/min. The reported values are peak values. ¹H NMR spectra were recorded with Bruker Avance DPX 400 and 360 spectrometers, and chemical shifts (δ) are expressed in parts per million (ppm) with TMS as internal standard. Mass spectral data were obtained via GC–MS analysis, using an Agilent 6890 series GC combined with a 5973N mass selected detector. High resolution mass spectra were acquired on a Acquity UPLC/QToF Premier system (Waters). The mass spectrometer was equipped with an ESI source and was operated in the positive ion mode. Leucine enkephalin was used as external lock spray. The source temperature was 120 °C, desolvation temperature was 350 °C, and the cone voltage was set to 30 V. Elemental analyses were performed with a Carlo-Erba EA1110 analyzer. Combustion analytical results were within 0.4% of the theoretical values except when noted otherwise. For all tested and final compounds where no analytical purity is mentioned, compounds were confirmed to be >95% pure via HPLC methods. The analytical LC measurement was performed using an Acquity UPLC (Waters) system comprising a binary pump, a sample organizer, a column heater (set at 55 °C), a diode-array detector (DAD), and a bridged ethylsiloxane/silica hybrid (BEH) C18 column (1.7 μ m, 2.1 mm \times 50 mm; Waters Acquity) with a flow rate of 0.8 mL/min. Two mobile phases (mobile phase A consisting of 0.1% formic acid in H₂O/methanol 95/5; mobile phase B consisting of methanol) were used to run a gradient condition from 95% A and 5% B to 5% A and 95% B in 1.3 min and held for 0.2 min. An injection volume of 0.5 μ L was used. Cone voltage was 10 V for positive ionization mode and 20 V for negative ionization mode. Flow from the column was split to a mass spectrometer. The MS detector was configured with an electrospray ionization source. Mass spectra were acquired by scanning from 100 to 1000 in 0.18 s using a dwell

time of 0.02 s. The capillary needle voltage was 3.5 kV, and the source temperature was maintained at 140 °C. Nitrogen was used as the nebulizer gas. Sensitive reactions were performed under nitrogen. Commercial solvents were used without any pretreatment. Preparative HPLC purifications were carried out using a Shandon Hyperprep column C18 BDS (base deactivated silica), 8 μ m, 250 g, 5 cm i.d., eluting with a gradient of three subsequent mobile phases: phase A consisting of a 0.25% NH₄HCO₃ solution in water; phase B consisting of CH₃OH; phase C consisting of CH₃CN).

In general, final compounds obtained as solids were triturated with DIPE. Alternatively, some compounds were precipitated and isolated as the HCl salt, by dissolving them in diethyl ether followed by the addition of a 1 N HCl solution in diethyl ether.

Allyl isothiocyanate (AITC), benzyl isothiocyanate (BITC), acrolein, 1-chloroacetophenone (CN), ethyl bromoacetate, and compounds **51**, **52**, **55**, **56** were purchased from Sigma-Aldrich. Fluperlapine (**53**) was purchased from Sanver Tech. 2-Chlorobenzylidene malononitrile (CS), **54**, and **57** were purchased from Scientific Exchange. Bromobenzyl cyanide¹⁹ morphanthridine,²⁰ CR,²¹ **58**,¹³ and **59**¹³ were synthesized according to literature procedures. All compounds were dissolved in dimethyl sulfoxide (DMSO) as 5, 10, or 100 mM stock solutions which were used within 48 h of their preparation.

CAUTION: All active TRPA1 agonist compounds mentioned in this article should be handled with care in a fumehood, using gloves, because of their strong irritant and lachrymatory properties.

5H-Dibenzo[b,e]azepine-10-carboxylic Acid Methyl Ester (6). **Step 1. 2-(3-Bromophenyl)-1,4-dihydro-2H-benzo[d][1,3]oxazine (14a).** A mixture of 2-(hydroxymethyl)aniline (9.0 g, 73 mmol) and 3-bromobenzaldehyde (13.5 g, 73 mmol) in 2-propanol (100 mL) was stirred for 3 h at room temperature. The solvent was evaporated, and the residue (20.5 g, 97%) was used as such in the next step. Part (3 g) of the residue was crystallized from hexane. The precipitate was filtered off and dried in vacuo, yielding 1.37 g of intermediate **14a**; mp 53.6 °C. ¹H NMR (360 MHz, DMSO-*d*₆) δ ppm 4.76 (d, *J* = 14.6 Hz, 1 H), 4.99 (d, *J* = 14.6 Hz, 1 H), 5.59 (d, *J* = 3.3 Hz, 1 H), 6.43 (d, *J* = 2.9 Hz, 1 H), 6.68 (d, *J* = 7.7 Hz, 2 H), 6.91 (d, *J* = 7.3 Hz, 1 H), 7.01 (t, *J* = 7.7 Hz, 1 H), 7.39 (t, *J* = 7.9 Hz, 1 H), 7.53 (d, *J* = 8.1 Hz, 1 H), 7.60 (d, *J* = 8.1 Hz, 1 H), 7.70 (s, 1 H).

Step 2. [2-(3-Bromobenzylamino)phenyl]methanol (15a). Sodium borohydride (4.4 g, 0.12 mol) was added slowly to a mixture of **14a** (17.1 g, 59 mmol) in dry ethanol (200 mL) under a nitrogen atmosphere. The reaction mixture was stirred and heated at reflux for 1 h. The mixture was cooled on an ice–water bath, quenched with a 20% aqueous NH₄Cl solution, and extracted with CH₂Cl₂. The organic layer was dried over MgSO₄, filtered, and concentrated under reduced pressure to give 14.8 g (86%) of crude **15a**. ¹H NMR (360 MHz, DMSO-*d*₆) δ ppm 4.37 (d, *J* = 6.2 Hz, 2 H), 4.49 (d, *J* = 5.5 Hz, 2 H), 5.17 (t, *J* = 5.5 Hz, 1 H), 5.83 (t, *J* = 6.0 Hz, 1 H), 6.40 (d, *J* = 8.1 Hz, 1 H), 6.54 (t, *J* = 7.3 Hz, 1 H), 6.98 (dd, *J* = 15.4, 1.5 Hz, 1 H), 7.10 (d, *J* = 7.3 Hz, 1 H), 7.28 (d, *J* = 8.1 Hz, 1 H), 7.37 (d, *J* = 7.7 Hz, 1 H), 7.41 (dd, *J* = 8.1, 1.83 Hz, 1 H), 7.54 (s, 1 H).

Step 3. 10-Bromo-6,11-dihydro-5H-dibenzo[b,e]azepine (16a) and 8-Bromo-6,11-dihydro-5H-dibenzo[b,e]azepine (16b). A solution of **15a** (52.6 g, 0.18 mol) in CH₂Cl₂ (50 mL) was added over a 1 h period to a cooled (–10 to –20 °C) solution of concentrated H₂SO₄ (500 mL). Then the ice bath was removed, and the mixture was stirred for 1 h at room temperature. The reaction mixture was added to ice–water, cooled on ice, and alkalized with a 50% aqueous NaOH solution. The resulting mixture (\pm 3 L) was extracted with CH₂Cl₂. The organic layer was separated, dried over MgSO₄, filtered, and the filtrate was concentrated in vacuo. The residue (47 g) was partly (8 g) purified via supercritical fluid chromatography (SFC, column Diacel AD-H 30 mm \times 250 mm, mobile phase of 55% MeOH/45% CO₂ + 0.2% isopropylamine, 40 °C, 100 bar) to give 2 g

(24%) of **16a** and 4.65 g (55%) of **16b**. Data for **16a**: mp 100.9 °C. ¹H NMR (360 MHz, DMSO-*d*₆) δ ppm 4.33 (s, 2 H), 4.47 (d, *J* = 5.1 Hz, 2 H), 5.98 (t, *J* = 5.1 Hz, 1 H), 6.35–6.42 (m, 2 H), 6.84 (td, *J* = 7.7, 1.5 Hz, 1 H), 6.89 (dd, *J* = 7.7, 1.5 Hz, 1 H), 7.13 (t, *J* = 8.1 Hz, 1 H), 7.25 (dd, *J* = 7.7, 1.5 Hz, 1 H), 7.51 (dd, *J* = 8.1, 1.1 Hz, 1 H). Data for **16b**: mp 135.5 °C. ¹H NMR (360 MHz, DMSO-*d*₆) δ ppm 4.09 (s, 2 H), 4.39 (d, *J* = 5.1 Hz, 2 H), 5.92 (t, *J* = 5.1 Hz, 1 H), 6.38 (t, 2 H), 6.82 (td, *J* = 7.7, 1.5 Hz, 1 H), 6.88 (d, *J* = 7.3 Hz, 1 H), 7.20 (d, *J* = 8.1 Hz, 1 H), 7.39 (dd, *J* = 8.1, 2.2 Hz, 1 H), 7.46 (d, *J* = 2.2 Hz, 1 H).

Step 4. 6,11-Dihydro-5H-dibenzo[*b,e*]azepine-10-carboxylic Acid Methyl Ester (18a). A mixture of **16a** (2.2 g, 8.0 mmol), KOAc (4 g, 41 mmol), Pd(OAc)₂ (40 mg, 0.2 mmol), and 1,3-bis(diphenylphosphino)propane (0.16 g, 0.4 mmol) in methanol (100 mL) and THF (100 mL) was placed in a pressure reactor and pressurized with CO gas up to 50 bar. The reaction mixture was heated at 125 °C for 16 h, then cooled, filtered over dicalite, and the solvent was evaporated. The residue was partitioned between CH₂Cl₂ and water. The organic layer was dried over MgSO₄, filtered, and then the filtrate was concentrated. The residue was purified by flash chromatography over silica gel (eluent, CH₂Cl₂). The desired fractions were collected and the solvent was evaporated, yielding 1.86 g (92%) of **18a**; mp 105.7 °C. ¹H NMR (400 MHz, CDCl₃) δ ppm 3.93 (s, 3 H), 4.58 (s, 3 H), 4.61 (s, 2 H), 6.37 (d, *J* = 8.1 Hz, 1 H), 6.60 (t, *J* = 6.8 Hz, 1 H), 6.94 (t, *J* = 8.4 Hz, 1 H), 7.12 (d, *J* = 7.3 Hz, 1 H), 7.23 (t, *J* = 7.7 Hz, 1 H), 7.34 (d, *J* = 7.3 Hz, 1 H), 7.77 (dd, *J* = 8.1, 1.5 Hz, 1 H). Anal. (C₁₆H₁₅NO₂) C, H, N.

Step 5. General MnO₂ Oxidation Procedure: 11H-Dibenzo[*b,e*]azepine-10-carboxylic Acid Methyl Ester (6). A mixture of **18a** (1.86 g, 74 mmol) and manganese oxide (3.2 g, 37 mmol) in toluene (20 mL) was stirred at 90 °C for 4 h. The reaction mixture was filtered over a silica gel pad (eluent, toluene and then CH₂Cl₂). The organic layer was concentrated. The residue was purified by flash chromatography over silica gel (eluent, heptane/EtOAc 100/0 to 70/30). The product fractions were collected, and the solvent was evaporated. The residue was triturated with diisopropyl ether, filtered off, and dried, yielding 1.35 g (73%) of **6**; mp 86.7 °C. ¹H NMR (360 MHz, CDCl₃) δ ppm 4.01 (3 H, s), 4.06 (2 H, br s), 7.25–7.33 (2 H, m), 7.36 (1 H, t, *J* = 7.7 Hz), 7.40–7.44 (1 H, m), 7.49–7.53 (1 H, m), 7.65 (1 H, dd, *J* = 7.7, 1.1 Hz), 8.01 (1 H, dd, *J* = 7.9, 1.3 Hz), 8.96 (1 H, s); ¹³C NMR (90 MHz, DMSO-*d*₆) δ ppm 33.05 (t), 52.39 (q), 125.52 (d), 126.22 (d), 127.04 (d), 127.07 (d), 127.98 (d), 128.24 (s), 131.82 (d), 131.97 (s), 132.24 (d), 133.32 (s), 139.83 (s), 145.21 (s), 159.84 (d), 167.14 (s); MS (EI⁺) *m/z* (rel intensity) 251 (99%, M⁺), 236 (66%), 220 (15%), 208 (5%), 191 (100%), 165 (22%); ESI-HRMS, found 252.1041, calculated for C₁₆H₁₄NO₂ (M + H)⁺ 252.1025. Anal. (C₁₆H₁₃NO₂) C, H, N.

6,11-Dihydro-5H-dibenzo[*b,e*]azepine-8-carboxylic Acid Methyl Ester (18b) and 11H-dibenzo[*b,e*]azepine-8-carboxylic Acid Methyl Ester (24). A mixture of **16b** (2.74 g, 10 mmol), 1,1'-(1,3-propanediyl)bis[1,1-diphenylphosphine] (80 mg, 0.2 mmol), Pd(OAc)₂ (20 mg, 0.08 mmol), and triethylamine (4 mL) in methanol (50 mL) and THF (50 mL) was stirred in an autoclave at 125 °C for 16 h under 50 atm of carbonmonoxide pressure, then for 4 h at 150 °C. The reaction mixture was cooled and filtered over dicalite. The solvent was evaporated, and the residue was purified via reversed phase HPLC. The desired fraction was collected and the solvent was evaporated, yielding 830 mg (33%) of **18b** and 380 mg (15%) of **24**. Data for **18b**: mp 155 °C. ¹H NMR (400 MHz, CDCl₃) δ ppm 3.90 (s, 3 H), 4.09 (br s, 1 H), 4.22 (s, 2 H), 4.54 (s, 2 H), 6.42 (dd, *J* = 8.1, 0.7 Hz, 1 H), 6.61 (td, *J* = 7.3, 1.1 Hz, 1 H), 6.94–7.00 (m, 2 H), 7.30 (d, *J* = 7.8 Hz, 1 H), 7.86 (d, *J* = 1.5 Hz, 1 H), 7.90 (dd, *J* = 7.7, 1.8 Hz, 1 H). Anal. (C₁₆H₁₅NO₂) C, H, N. Data for **24**: mp 137.9 °C. ¹H NMR (360 MHz, CDCl₃) δ ppm 3.76 (2 H, s), 3.93 (3 H, s), 7.24–7.27 (2 H, m), 7.28–7.33 (1 H, m), 7.39 (1 H, d, *J* = 8.1 Hz), 7.42 (1 H, d, *J* = 7.7 Hz), 8.10 (1 H, dd, *J* = 8.1, 1.8 Hz), 8.18 (1 H, d, *J* = 1.5 Hz), 8.94 (1 H, s); ¹³C NMR (90 MHz, DMSO-*d*₆) δ ppm 37.97 (t), 52.65 (q), 126.46 (d), 127.68 (d), 127.71 (d), 128.01 (d), 128.44 (s), 128.50 (d),

129.75 (d), 132.27 (d), 132.29 (s), 145.57 (s), 146.45 (s), 160.26 (d), 165.95 (s); MS (EI⁺) *m/z* (rel intensity) 251 (100%, M⁺), 236 (3%), 220 (22%), 192 (35%), 165 (26%); ESI-HRMS, found 252.1035, calculated for C₁₆H₁₄NO₂ (M + H)⁺ 252.1025. Anal. (C₁₆H₁₃NO₂ 0.4 H₂O) C, H, N.

Dibenzo[*b,f*][1,4]oxazepine-4-carboxylic Acid Methyl Ester (32). **Step 1. 3-Bromo-2-fluoro-*N*-(2-hydroxyphenyl)benzamide 27a.** A mixture of 3-bromo-2-fluorobenzoic acid (5.0 g, 22 mmol) and SOCl₂ (20 mL) was stirred and refluxed for 2 h. The reaction mixture was concentrated in vacuo and coevaporated twice with toluene. The crude acid chloride residue was dissolved in THF (25 mL) and was added dropwise to a mixture of 2-aminophenol (2.4 g, 22 mmol) and triethylamine (4.5 g, 44 mmol) in THF (75 mL) at 0 °C. The reaction mixture was allowed to warm to room temperature and stirred overnight. The reaction mixture was poured into water (400 mL) and acidified to pH 4–5 with a 1 N aqueous HCl solution. The precipitate was filtered off and washed with a 1 N aqueous HCl solution and water, dried in vacuo, yielding 6.4 g (93%) of **27a**; mp 219.3 °C. ¹H NMR (360 MHz, DMSO-*d*₆) δ ppm 6.83 (t, *J* = 7.6 Hz, 1 H), 6.92 (d, *J* = 8.8 Hz, 1 H), 7.02 (t, *J* = 7.6 Hz, 1 H), 7.30 (t, *J* = 7.9 Hz, 1 H), 7.78 (t, *J* = 7.1 Hz, 1 H), 7.89 (t, *J* = 7.4 Hz, 1 H), 7.94 (d, *J* = 7.9 Hz, 1 H), 9.61 (d, *J* = 4.9 Hz, 1 H), 9.96 (s, 1 H).

Step 2. 4-Bromo-10H-dibenzo[*b,f*][1,4]oxazepin-11-one (28a). A mixture of **27a** (3.8 g, 12 mmol) and sodium hydroxide (490 mg, 12 mmol) in DMF (60 mL) was stirred and refluxed for 5 h. The reaction mixture was poured onto 800 mL of ice–water and the resulting precipitate filtered off and washed with a 1 N aqueous sodium hydroxide solution and water, then dried in vacuo, yielding 2.5 g (70%) of **28a**; mp 272.3 °C. ¹H NMR (360 MHz, DMSO-*d*₆) δ ppm 7.13 (t, *J* = 7.7 Hz, 1 H), 7.18 (dd, *J* = 8.1, 1.8 Hz, 1 H), 7.37 (td, *J* = 7.7, 1.1 Hz, 1 H), 7.44 (dd, *J* = 7.7, 1.8 Hz, 1 H), 7.47 (dd, *J* = 8.4, 1.1 Hz, 1 H), 7.67 (td, *J* = 8.1, 1.8 Hz, 1 H), 7.81 (dd, *J* = 7.7, 1.8 Hz, 1 H), 10.72 (s, 1 H).

Step 3. 4-Bromo-10,11-dihydrodibenzo[*b,f*][1,4]oxazepine (29a). To a suspension of **28a** in THF (80 mL) was added a 1 M BH₃ solution in THF (24 mL, 24 mmol), and the reaction mixture was stirred at room temperature for 2 weeks. The reaction mixture was cooled on ice, and 100 mL of a 1 N aqueous HCl solution was added. The mixture was partially concentrated in vacuo and then basified with solid NaHCO₃ (pH ~7). The aqueous layer was extracted with 2 × 150 mL of CH₂Cl₂. The separated organic layer was dried over MgSO₄, filtered, and the filtrate was concentrated. The residue was purified via reversed phase HPLC, yielding 2.1 g (85%) of **29a**; mp 254 °C. ¹H NMR (360 MHz, DMSO-*d*₆) δ ppm 4.43 (d, *J* = 4.3 Hz, 2 H), 6.17 (t, *J* = 4.3 Hz, 1 H), 6.52 (td, *J* = 7.6, 1.6 Hz, 1 H), 6.57 (dd, *J* = 8.1, 1.6 Hz, 1 H), 6.82 (td, *J* = 7.4, 1.7 Hz, 1 H), 7.07 (t, *J* = 7.7 Hz, 1 H), 7.12 (dd, *J* = 7.7, 1.5 Hz, 1 H), 7.35 (dd, *J* = 7.5, 1.3 Hz, 1 H), 7.58 (dd, *J* = 8.1, 1.5 Hz, 1 H).

Step 4. 10,11-Dihydrodibenzo[*b,f*][1,4]oxazepine-4-carboxylic Acid Methyl Ester (30a). A 75 mL stainless steel autoclave was charged under nitrogen atmosphere with **29a** (725 mg, 2.6 mmol), Pd(OAc)₂ (10 mg, 0.04 mmol), 1,3-bis(diphenylphosphino)propane (40 mg, 0.1 mmol), KOAc (750 mg, 7.9 mmol), methanol (20 mL), and THF (20 mL). The autoclave was closed and pressurized to 50 atm. CO and the reaction was carried out for 16 h at 125 °C. The reaction mixture was filtered and concentrated in vacuo. The residue was partitioned between CH₂Cl₂ and water. The separated organic layer was dried over MgSO₄, filtered, and the filtrate was concentrated. The residue was purified by silica gel flash chromatography (eluent heptane/CH₂Cl₂ 70/30 to 0/100), yielding 550 mg (82%) of **30a** as a light yellow oil. ¹H NMR (360 MHz, DMSO-*d*₆) δ ppm 3.89 (s, 3 H), 4.43 (d, *J* = 4.2 Hz, 2 H), 6.13 (t, *J* = 4.2 Hz, 1 H), 6.51 (td, *J* = 7.7, 1.5 Hz, 1 H), 6.56 (dd, *J* = 8.1, 1.5 Hz, 1 H), 6.80 (td, *J* = 7.7, 1.5 Hz, 1 H), 7.04 (dd, *J* = 8.1, 1.5 Hz, 1 H), 7.22 (t, *J* = 7.7 Hz, 1 H), 7.55 (dd, *J* = 7.7, 1.8 Hz, 1 H), 7.65 (dd, *J* = 7.7, 1.8 Hz, 1 H).

Step 5. Dibenzo[*b,f*][1,4]oxazepine-4-carboxylic Acid Methyl Ester, HCl Salt (32). A mixture of **30a** (510 mg, 2.0 mmol) and

MnO₂ (521 mg, 6.0 mmol) in toluene (20 mL) was stirred at 80 °C for 3 h. The reaction mixture was filtered over a dicalite pad (eluent toluene, then CH₂Cl₂). The organic layer was concentrated, and the residue was purified by silica gel flash chromatography (eluent CH₂Cl₂/CH₃OH(NH₃) 100/0 to 99/1). The pure fractions were collected, and the solvent was evaporated. The residue was purified further via reversed phase HPLC. The product was dissolved in Et₂O (10 mL), a 2 N HCl solution in Et₂O was added, and the resulting precipitate was filtered off and dried, yielding 305 mg (53%) of **32** as a yellow solid; mp 205.5 °C. ¹H NMR (360 MHz, DMSO-*d*₆) δ ppm 3.96 (3 H, s), 7.27–7.33 (1 H, m), 7.35–7.41 (3 H, m), 7.44 (1 H, t, *J* = 7.9 Hz), 7.84 (1 H, dd, *J* = 7.7, 1.5 Hz), 7.94 (1 H, dd, *J* = 7.9, 1.6 Hz), 8.75 (1 H, s); ¹³C NMR free base (90 MHz, DMSO-*d*₆) δ ppm 52.91 (q), 122.26 (d), 124.33 (s), 125.84 (d), 126.63 (d), 128.69 (s), 128.93 (d), 129.40 (d), 134.35 (d), 134.69 (d), 140.68 (s), 152.17 (s), 157.74 (s), 160.72 (d), 165.30 (s); MS (EI⁺) *m/z* (rel intensity) 253 (100%, M⁺), 222 (56%), 194 (11%), 166 (14%); ESI-HRMS, found 254.0833 calculated for C₁₅H₁₂NO₃ (M + H)⁺ 254.0817. Anal. (C₁₅H₁₁NO₃·HCl) C, H, N.

Dibenzo[*b,f*][1,4]oxazepine-4-carbonitrile (38). Step 1. 10,1-Dihydrodibenzo[*b,f*][1,4]oxazepine-4-carbonitrile (33a). A mixture of **29a** (750 mg, 2.7 mmol) and CuCN (608 mg, 6.8 mmol) in DMF (15 mL) was degassed and then shaken under nitrogen atmosphere at 140 °C overnight. The reaction mixture was cooled to room temperature, and a 0.2 N aqueous sodium hydroxide solution (200 mL) was added. The mixture was extracted twice with ethyl acetate (2 × 100 mL). The combined organic layers were washed with water and brine, dried over MgSO₄, concentrated in vacuo, yielding 255 mg (42%) of intermediate **33a**. ¹H NMR (360 MHz, DMSO-*d*₆) δ ppm 4.45 (d, *J* = 4.1 Hz, 2 H), 6.23 (t, *J* = 4.0 Hz, 1 H), 6.60 (td, *J* = 8.1, 1.5 Hz, 1 H), 6.65 (dd, *J* = 8.1, 1.5 Hz, 1 H), 6.87 (td, *J* = 7.7, 1.5 Hz, 1 H), 7.04 (dd, *J* = 8.1, 1.5 Hz, 1 H), 7.30 (t, *J* = 7.7 Hz, 1 H), 7.69 (dd, *J* = 7.7, 1.5 Hz, 1 H), 7.77 (dd, *J* = 7.7, 1.5 Hz, 1 H).

Step 2. Dibenzo[*b,f*][1,4]oxazepine-4-carbonitrile (38). Starting from **33a**, standard MnO₂ oxidation gave compound **31** in 36% yield: mp 109.3 °C. ¹H NMR (360 MHz, DMSO-*d*₆) δ ppm 7.25 (dd, *J* = 7.3, 1.8 Hz, 1 H), 7.34 (td, *J* = 7.3, 1.8 Hz, 1 H), 7.39–7.44 (m, 2 H), 7.53 (t, *J* = 7.7 Hz, 1 H), 7.95 (dd, *J* = 7.7, 1.8 Hz, 1 H), 8.08 (dd, *J* = 7.7, 1.8 Hz, 1 H), 8.71 (s, 1 H). Anal. (C₁₄H₈N₂O) C, H, N.

Dibenzo[*b,f*][1,4]oxazepine-4-carboxylic Acid Amide (41). A mixture of **38** (60 mg, 0.27 mmol) and concentrated H₂SO₄ (2 mL) was stirred at a temperature between 0 and 5 °C for 2 h. The mixture was kept stirring at room temperature for 3 days. The reaction mixture was poured into 100 mL of ice–water and basified with a concentrated aqueous NH₃ solution. The mixture was extracted with CH₂Cl₂. The organic layer was washed with brine, dried over MgSO₄, filtered, and the filtrate was concentrated. Yield 64 mg (99%) of **41**; mp 193 °C. ¹H NMR (360 MHz, DMSO-*d*₆) δ ppm 7.21–7.29 (m, 2 H), 7.31–7.38 (m, 3 H), 7.66 (dd, *J* = 7.7, 1.8 Hz, 1 H), 7.69 (dd, *J* = 7.7, 1.8 Hz, 1 H), 7.74 (br s, 1 H), 7.96 (br s, 1 H), 8.68 (s, 1 H). Anal. (C₁₄H₁₀N₂O₂) C, H, N.

Biology. Cells and Culture. T-REx-293 cells (Invitrogen, Belgium) were stably transfected with the tetracycline-inducible human TRPA1 gene and cultured as previously described.⁸ Briefly, hTRPA1/T-REx-HEK293 cells (referred to as hTRPA1-HEK cells in the text) were maintained under standard sterile cell culture conditions. The culture medium for the hTRPA1-HEK cells was Dulbecco's modified Eagle's medium (DMEM, Gibco BRL, Invitrogen, Belgium) supplemented with 0.5 g/L Geneticin (G148, Gibco), 5 mg/L blasticidin (Invitrogen), 14.6 g/L L-glutamine (200 mM, Gibco), 5 g/L penicillin/streptomycin (5 × 10^{−6} IU/L, Gibco), 5.5 g/L pyruvic acid (Gibco), and 10% fetal calf serum (Hyclone).

Ca²⁺ Fluorometry. For the fluorometric Ca²⁺ measurements hTRPA1-HEK cells were resuspended in seeding medium: Hanks' balanced salt solution (HBSS with CaCl₂ and MgCl₂;

Gibco) supplemented with 14.6 g/L L-glutamine (200 mM), 5 g/L penicillin/streptomycin (5 × 10^{−6} IU/L), 5.5 g/L pyruvic acid, 5 mM HEPES (Gibco), 5 mL of insulin-transferrin-selenium-x (Gibco), and 10% fetal calf serum (heat inactivated for 30 min at 56 °C). The cells were seeded in poly-D-lysine-coated 384-well round-bottom polypropylene plates (Costar Corning, Data Packaging) at 12 000 cells/well. Then 50 ng/mL tetracycline was added to induce the hTRPA1 expression 24 h before the experiment. The cells were loaded with 5 mg/L Fluo4-AM (Molecular Probes, Invitrogen, Belgium) dissolved in HBSS seeding medium supplemented with 0.7 g/L probenecid (Sigma) and incubated for 1 h at 37 °C and subsequently at 20 °C for 1–2 h. The fluorescence was measured in the FDSS 6000 imaging based plate reader (Hamamatsu Photonics K.K., Japan). The excitation wavelength was 488 nm and the emission wavelength 540 nm. After a control period of 12 s the TRPA1 agonists were added and their effect was measured within 14 min after application. The mean and SEM of four repeats at each concentration were plotted as a function of the agonist concentration, and the concentration response data were fitted to obtain the EC₅₀ value.

Electrophysiological Measurements. For patch clamp experiments the cells were resuspended in culture medium without Geneticin and blasticidin but with 500 ng/mL tetracycline to induce the hTRPA1 expression. The cells were seeded in Nunclon Petri dishes (35 mm, Nunc, Denmark) at 30 000 cells/mL and incubated in a humidified incubator at 37 °C with 5% CO₂ for 2–5 days before the experiments. Whole cell patch clamp recordings were performed as described⁸ with an EPC9 or EPC10 amplifier (HEKA Elektronik, Germany). Gigaseals were obtained, and the series resistance was compensated for 90%. The membrane potential was clamped at −30 mV throughout the experiment, and fast solution changes were done by means of a Warner SF-77B fast step superfusion system (Warner Instruments LLC). Currents were sampled at 10 kHz and filtered at 1 kHz. Data acquisition was done with Pulse/Pulsefit (HEKA Elektronik, Germany). The extracellular solution contained (in mM) 152 NaCl, 3 KCl, 10 glucose, 10 HEPES, 1 MgCl₂, and 2 CaCl₂, and the pH was adjusted to 7.4 with NaOH. The intracellular solution contained (in mM) 130 CsCl, 10 EGTA, 10 HEPES, 2 MgATP, 0.2 Na₃GTP, and 6.5 CaCl₂, and the pH was adjusted to 7.2 with CsOH. The free Ca²⁺ concentration of the intracellular solution was 311 nM (calculated with MaxChelator, free at <http://www.stanford.edu/~cpatton/maxc.html>). A good control of the intracellular Ca²⁺ concentration was necessary because of the direct activation of hTRPA1 channels by Ca²⁺.²² At the end of the experiments 50 μM TRPA1 blocker ruthenium red was applied to evaluate the non-TRPA1 component of the holding current and as a consequence the quality of the experiment. For electrophysiological experiments the stock solutions of the compounds (10 or 100 mM) were further diluted in DMSO. The final DMSO concentration in the extracellular solution was 0.1%. Ruthenium red was dissolved at 50 μM in extracellular solution containing 0.1% DMSO.

Acknowledgment. We thank Sebastiaan van Liempt for carrying out the glutathione trapping experiments.

Supporting Information Available: Synthesis and analytical data of all intermediates and compounds not described in the Experimental Section, description of the electrophysiological effect of **6** on the hTRPA1 current to illustrate how dose response curves in Figure 1 have been obtained, and experimental procedures on metabolic stability and reactive metabolite formation experiments. This material is available free of charge via the Internet at <http://pubs.acs.org>.

References

- (1) Recent reviews: (a) Patapoutian, A.; Tate, S.; Woolf, C. J. Transient receptor potential channels: targeting pain at the source.

- Nat. Rev. Drug Discovery* **2009**, *8*, 55–68. (b) Baraldi, P. G.; Preti, D.; Materazzi, S.; Geppetti, P. Transient receptor potential ankyrin 1 (TRPA1) channel as emerging target for novel analgesics and anti-inflammatory agents. *J. Med. Chem.* **2010**, *53*, 5085–5107.
- (2) Viana, F.; Ferrer-Montiel, A. TRPA1 modulators in preclinical development. *Expert Opin. Ther. Pat.* **2009**, *19*, 1787–1799.
 - (3) (a) Cai, X. A new tr(i)p to sense pain: TRPA1 channel as a target for novel analgesics. *Expert Rev. Neurother.* **2008**, *8*, 1675–1681. (b) Bang, S.; Hwang, S. W. Polymodal ligand sensitivity of TRPA1 and its modes of interactions. *J. Gen. Physiol.* **2009**, *133*, 257–262.
 - (4) (a) Bessac, B. F.; Jordt, S. E. Breathing TRP channels: TRPA1 and TRPV1 in airway chemosensation and reflex control. *Physiology* **2008**, *23*, 360–370. (b) Caceres, A. I.; Brackmann, M.; Elia, M. D.; Bessac, B. F.; del Camino, D.; D'Amours, M.; Witek, J. S.; Fanger, C. M.; Chong, J. A.; Hayward, N. J.; Homer, R. J.; Cohn, L.; Huang, X.; Moran, M. M.; Jordt, S. E. A sensory neuronal channel essential for airway inflammation and hyperreactivity in asthma. *Proc. Natl. Acad. Sci. U.S.A.* **2009**, *106*, 9099–9104.
 - (5) Everaerts, W.; Gevaert, T.; Nilius, B.; De Ridder, D. On the origin of bladder sensing: Tr(i)p(s) in urology. *NeuroUrol. Urodyn.* **2008**, *27*, 264–273.
 - (6) (a) Bautista, D. M.; Movahed, P.; Hinman, A.; Axelsson, H. E.; Sterner, O.; Hogestatt, E. D.; Julius, D.; Jordt, S. E.; Zygmunt, P. M. Pungent products from garlic activate the sensory ion channel TRPA1. *Proc. Natl. Acad. Sci. U.S.A.* **2005**, *102*, 12248–12252. (b) Jordt, S. E.; Bautista, D. M.; Chuang, H. H.; McKemy, D. D.; Zygmunt, P. M.; Hogestatt, E. D.; Meng, I. D.; Julius, D. Mustard oils and cannabinoids excite sensory nerve fibres through the TRP channel ANKTM1. *Nature* **2004**, *427*, 260–265. (c) Macpherson, L. J.; Geierstanger, B. H.; Viswanath, V.; Bandell, M.; Eid, S. R.; Hwang, S.; Patapoutian, A. The pungency of garlic: activation of TRPA1 and TRPV1 in response to allicin. *Curr. Biol.* **2005**, *15*, 929–934.
 - (7) (a) Hinman, A.; Chuang, H. H.; Bautista, D. M.; Julius, D. TRP channel activation by reversible covalent modification. *Proc. Natl. Acad. Sci. U.S.A.* **2006**, *103*, 19564–19568. (b) Macpherson, L. J.; Dubin, A. E.; Evans, M. J.; Marr, F.; Schultz, P. G.; Cravatt, B. F.; Patapoutian, A. Noxious compounds activate TRPA1 ion channels through covalent modification of cysteines. *Nature* **2007**, *445*, 541–545.
 - (8) Brône, B.; Peeters, P. J.; Marrannes, M.; Mercken, M.; Nuydens, R.; Meert, T.; Gijssen, H. J. M. Tear gasses CN, CR, and CS are potent activators of the human TRPA1 receptor. *Toxicol. Appl. Pharmacol.* **2008**, *231*, 150–156.
 - (9) Blain, P. G. Tear gases and irritant incapacitants 1-chloroacetophenone, 2-chlorobenzylidene malononitrile and dibenz[b,f]-1,4-oxazepine. *Toxicol. Rev.* **2003**, *22*, 103–110.
 - (10) Bessac, B. F.; Sivula, M.; von Hehn, C. A.; Caceres, A. I.; Escalera, J.; Jordt, S.-E. Transient receptor potential ankyrin 1 antagonists block the noxious effects of toxic industrial isocyanates and tear gases. *FASEB J.* **2009**, *23*, 1102–1114.
 - (11) Andres, J. I.; Alcazar, J.; Alonso, J. M.; Diaz, A.; Fernandez, J.; Gil, P.; Iturrino, L.; Matesanz, E.; Meert, T. F.; Megens, A.; Sipido, V. K. Synthesis and structure–activity relationship of 2-(aminoalkyl)-2,3,3a,8-tetrahydrodibenzo[c,f]isoxazolo[2,3-a]azepine derivatives: a novel series of 5-HT(2A/2C) receptor antagonists. Part 2. *Bioorg. Med. Chem. Lett.* **2002**, *12*, 243–248.
 - (12) Hunziker, F.; Kunzle, F.; Schindler, O.; Schmutz, J. Seven-membered heterocycles. III. Dibenzazepines and oxazepines, and dibenzodiazepines and -thiazepines. *Helv. Chim. Acta* **1964**, *47*, 1163–1172.
 - (13) Brewster, K.; Clarke, R. J.; Harrison, J. M.; Inch, T. D.; Utley, D. Preparation of the eight monohydroxydibenz[b,f][1,4]oxazepin-11(10H)-ones. *J. Chem. Soc., Perkin Trans. 1* **1976**, 1286–1290.
 - (14) Liu, Y.; Lubin, M. L.; Reitz, T. L.; Wang, Y.; Colburn, R. W.; Flores, C. M.; Qin, N. Molecular identification and functional characterization of a temperature-sensitive transient receptor potential channel (TRPM8) from canine. *Eur. J. Pharmacol.* **2006**, *530*, 23–32.
 - (15) hTRPV1 and cTRPM8 agonism was determined using a modification of the methods described in the following: Behrendt, H.-J.; Germann, T.; Gillen, C.; Hatt, H.; Jostock, R. Characterization of the mouse cold menthol receptor TRPM8 and vanilloid receptor type-1 VR1 using a fluorometric imaging plate reader (FLIPR) assay. *Br. J. Pharmacol.* **2004**, *141*, 737–745.
 - (16) (a) Baillie, T. A. Metabolic activation and drug design: challenges and opportunities in chemical toxicology. *Chem. Res. Toxicol.* **2006**, *19*, 889–893. (b) Ma, S.; Subramanian, R. Detecting and characterizing reactive metabolites by liquid chromatography/tandem mass spectrometry. *J. Mass Spectrom.* **2006**, *41*, 1121–1139.
 - (17) Wen, B.; Fitch, W. L. Screening and characterization of reactive metabolites using glutathione ethyl ester in combination with Q-trap mass spectrometry. *J. Mass Spectrom.* **2009**, *44*, 90–100.
 - (18) Gijssen, H. J. M.; Berthelot, D. J.; De Cleyn, M. A. J. 3,4-Dihydropyrimidine Derivatives as TRPA1 Antagonists and Their Preparation, Pharmaceutical Compositions and Use in the Treatment of Diseases. WO2009147079, 2009.
 - (19) Molina, P.; Lopez-Leonardo, C.; Llamas-Botia, J.; Foces-Foces, C.; Fernandez-Castano, C. Unexpected Staudinger reaction of [alpha]-azidoacetonitriles [alpha]-phenyl substituted with triphenylphosphine. Preparation, X-ray crystal and molecular structures of a phosphazine, an aminophosphonium carbanion salt and a phosphazide, with (Z)-configuration. *Tetrahedron* **1996**, *52*, 9629–9642.
 - (20) Wardrop, A. W. H.; Sainsbury, G. L.; Harrison, J. M.; Inch, T. D. Preparation of some dibenz[b,f][1,4]oxazepines and dibenz[b,e]azepines. *J. Chem. Soc., Perkin Trans. 1* **1976**, 1279–1285.
 - (21) Fakhraian, H.; Nafary, Y.; Yarahmadi, A.; Hadj-Ghanbary, H. Improved etherification procedure for the preparation of dibenz[b,f]-[1,4]oxazepine. *J. Heterocycl. Chem.* **2008**, *45*, 1469–1472.
 - (22) Zurborg, S.; Yurgionas, B.; Jira, J. A.; Caspani, O.; Heppenstall, P. A. Direct activation of the ion channel TRPA1 by Ca²⁺. *Nat. Neurosci.* **2007**, *10*, 277–279.